



OPEN Detection and isolation of viable cancer cells mediated by spytag and spycatcher using conditionally replicative adenovirus and magnetic microbeads

Sadegh Goli^{1,4}, Maryam Kadkhodazadeh^{2,4}, Mahshid Kharaziha¹, Shaghayegh Haghooy Javanmard³ & Kayhan Azadmanesh⁴✉

Circulating tumor cells (CTCs) are critical biomarkers for cancer diagnosis, prognosis, and therapy monitoring, but their rarity and reliance on surface markers limit detection and isolation. While conditionally replicative adenoviruses (crADs) enable tumor-selective targeting, their use has been limited to fluorescence-based detection without robust isolation of viable cells. To overcome this, we developed a crAD-based platform integrating SpyTag/SpyCatcher technology with SpyCatcher-decorated magnetic microbeads for marker-independent CTC detection and isolation. The engineered adenovirus (CR-Ad5-ST-GFP) selectively replicates in telomerase-positive tumor cells, expressing green fluorescent protein (GFP) and SpyTag under independent promoters. By leveraging the SpyTag/SpyCatcher interaction, our platform isolates CTCs without relying on surface markers, addressing epithelial-to-mesenchymal transition (EMT) and phenotype variations. In proof-of-concept experiments, A-549 and Ca Ski cells spiked into peripheral blood mononuclear cells (PBMCs) at 1:10,000 were detected and isolated with over 80% efficiency. The isolated cells remained viable and were successfully re-cultured, demonstrating their potential for downstream applications such as molecular profiling and drug sensitivity testing. This method advances crAD-based approaches by combining tumor-selective viral targeting with marker-independent, viable CTC isolation. Its compatibility with microfluidic systems makes it a promising tool for tumor monitoring and personalized cancer treatment.

Keywords Circulating tumor cells (CTCs), Conditionally replicative adenovirus, SpyTag-SpyCatcher system, Detection and isolation, Cancer cells, Magnetic microbeads

Circulating tumor cells (CTCs) are malignant cells shed from primary or metastatic tumors into the bloodstream, playing a critical role in the metastatic cascade. Their detection and analysis offer a promising approach to non-invasive cancer diagnosis, prognosis, and therapeutic monitoring through liquid biopsy¹. However, the remarkable rarity of CTCs, often as few as one per billion blood cells, poses a substantial challenge for reliable identification and isolation². Furthermore, the phenotypic heterogeneity of CTCs, particularly during epithelial-mesenchymal transition (EMT), complicates their detection using conventional marker-based methods¹.

CTCs exhibit distinct biological characteristics, such as undergoing EMT, which aids in their release from the tumor and entry into circulation. Non-EMT CTCs retain epithelial markers like EpCAM and cytokeratins, making them detectable by conventional methods but less invasive. EMT CTCs lose these markers, gain mesenchymal traits like vimentin expression, and exhibit greater mobility, invasiveness, and therapy resistance. Their altered phenotype challenges traditional detection, highlighting the need for marker-independent methods. Detecting both types is crucial, as EMT CTCs drive metastasis, while non-EMT CTCs may transition later at metastatic

¹Department of Materials Engineering, Isfahan University of Technology, 84156-83111 Isfahan, Iran. ²ATMP Department, Breast Cancer Research Center, Motamed Cancer Institute, ACECR, Tehran, Iran. ³Metabolomics and Genomics Research Center, Cellular and Molecular Institute, Endocrinology and Metabolism Research Institute, Tehran University of Medical Sciences, Tehran, Iran. ⁴Molecular Virology Department, Pasteur Institute of Iran, Tehran, Iran. ✉email: azadmanesh@Pasteur.ac.ir; k.azadmanesh2@gmail.com

sites^{1,3,4}. Some CTCs travel as clusters, enhancing their metastatic potential, and display stem-like features that promote secondary tumor formation. Although many CTCs are eliminated in the bloodstream, a small fraction evade immune detection and successfully colonize distant organs^{1,3}.

Clinically relevant circulating tumor cells (CTCs) are identified based on several criteria, including the expression of epithelial markers (EpCAM, cytokeratins) and absence of leukocyte markers (CD45). Morphological traits like size and shape, along with genetic profiling for tumor-specific mutations (e.g., KRAS, EGFR) or telomerase activity, confirm malignancy. While their detection offers valuable clinical insights, the presence of CTCs alone does not always indicate active malignancy. Further clinical evaluation and monitoring are necessary to determine the significance of CTCs in individual patients^{3,5}.

Current CTC detection techniques primarily rely on immunoaffinity- and biophysical property-based approaches. Immunoaffinity-based methods, such as the FDA-approved CellSearch system, target epithelial markers like EpCAM or cytokeratins for CTC enrichment and detection. However, these methods are limited in detecting CTCs undergoing EMT, during which epithelial markers are downregulated, leading to false negatives and underestimating metastatic potential^{6,7}. Similarly, biophysical methods exploit differences in size, density, or deformability between CTCs and blood cells but suffer from low specificity, as some blood cells share overlapping properties with CTCs⁸. Moreover, most current methods fail to preserve cell viability, restricting their utility for downstream applications like molecular profiling and drug sensitivity testing⁹.

Recent advancements have explored alternative platforms, such as conditionally replicative adenoviruses (crADs), to address these limitations. These viruses selectively replicate in tumor cells with high telomerase activity, enabling the detection of viable CTCs independent of surface marker expression. This marker-independent approach holds significant potential for targeting CTCs that have undergone EMT, which often lose epithelial markers while maintaining telomerase activity, thus overcoming limitations of conventional detection methods¹⁰. For instance, OBP-401 (TelomeScan), an adenovirus engineered with an hTERT promoter-regulated E1A gene, has shown promise in selectively detecting telomerase-positive CTCs^{11,12}. However, traditional crAD platforms focus primarily on detection through fluorescence markers and do not integrate robust isolation systems, limiting their broader clinical applicability.

To overcome the limitations of traditional crAD platforms, this study introduces a novel approach that combines tumor-selective crADs with the SpyTag/SpyCatcher system and SpyCatcher-decorated agarose magnetic microbeads. The engineered adenovirus (CR-Ad5-ST-GFP) selectively replicates in telomerase-positive tumor cells, expressing green fluorescent protein (GFP) and SpyTag under independent promoters. SpyTag, a small peptide that forms a covalent bond with SpyCatcher, enables the robust and marker-independent isolation of CTCs, even in the absence of conventional epithelial markers. This design addresses key challenges posed by EMT and phenotypic heterogeneity in CTCs.

The SpyTag/SpyCatcher system offers several advantages over traditional antibody-based isolation methods. Unlike non-covalent interactions, which are prone to dissociation under harsh conditions, the SpyTag-SpyCatcher interaction forms a stable covalent bond that withstands mechanical forces, detergents, and extreme pH levels^{13,14}. This robust interaction ensures high efficiency in isolating viable CTCs while preserving their integrity for downstream applications such as re-culturing and genetic analysis. Additionally, using magnetic microbeads functionalized with SpyCatcher enables rapid and efficient cell separation from blood samples under physiologically favorable conditions¹⁵.

In this study, we developed and evaluated the CR-Ad5-ST-GFP platform for detecting and isolating CTCs from blood samples. Our approach leverages tumor-selective replication and marker-independent isolation, overcoming limitations associated with conventional methods that rely on epithelial markers or size-dependent separation. By utilizing a telomerase-dependent adenoviral system integrated with the SpyTag/SpyCatcher mechanism, our approach enables efficient and specific CTC capture while maintaining cell viability. This preserves viable candidate cells for potential downstream applications, including molecular profiling and drug sensitivity testing, highlighting its promise as a valuable tool for tumor monitoring and personalized oncology (Fig. 1).

Materials and methods

Cell lines

Three cancer cell lines—A-549 (non-small cell lung cancer, RRID: CVCL_0023), MCF-7 (breast cancer, RRID: CVCL_0031), and Ca Ski (cervical carcinoma)—along with 293AD cells (human embryonic kidney-derived, RRID: CVCL_KA63), were obtained from the National Cell Bank of the Pasteur Institute of Iran. The A-549 and MCF-7 cells were cultured in DMEM (Biosera, Philippines) supplemented with 10% fetal bovine serum (FBS) and 1% penicillin-streptomycin (Biosera, Philippines), while Ca Ski cells were maintained in RPMI 1640 under similar conditions. All cells were incubated at 37 °C with 5% CO₂ in a humidified atmosphere.

Plasmid construction and recombinant virus packaging

The adenoviral genome was engineered to include the E1A gene regulated by the hTERT promoter, ensuring selective replication in telomerase-positive cells. Two additional sequences—CMV-EGFP and CMV-SpyTag-Fc—were inserted into the E3 region of the genome. Detailed cloning procedures, including homologous recombination steps, are provided in the Supplementary Materials (Sections S1). Verification of the viral genome and successful packaging into CR-Ad5-ST-GFP was confirmed via PCR and titration analysis.

Replication potency and infectivity of CR-Ad5-ST-GFP

To evaluate viral replication, A-549 cells were seeded and infected with CR-Ad5-ST-GFP at an MOI of 10. After 24 and 48 h, GFP expression was monitored using fluorescence microscopy, and viral titers were quantified via

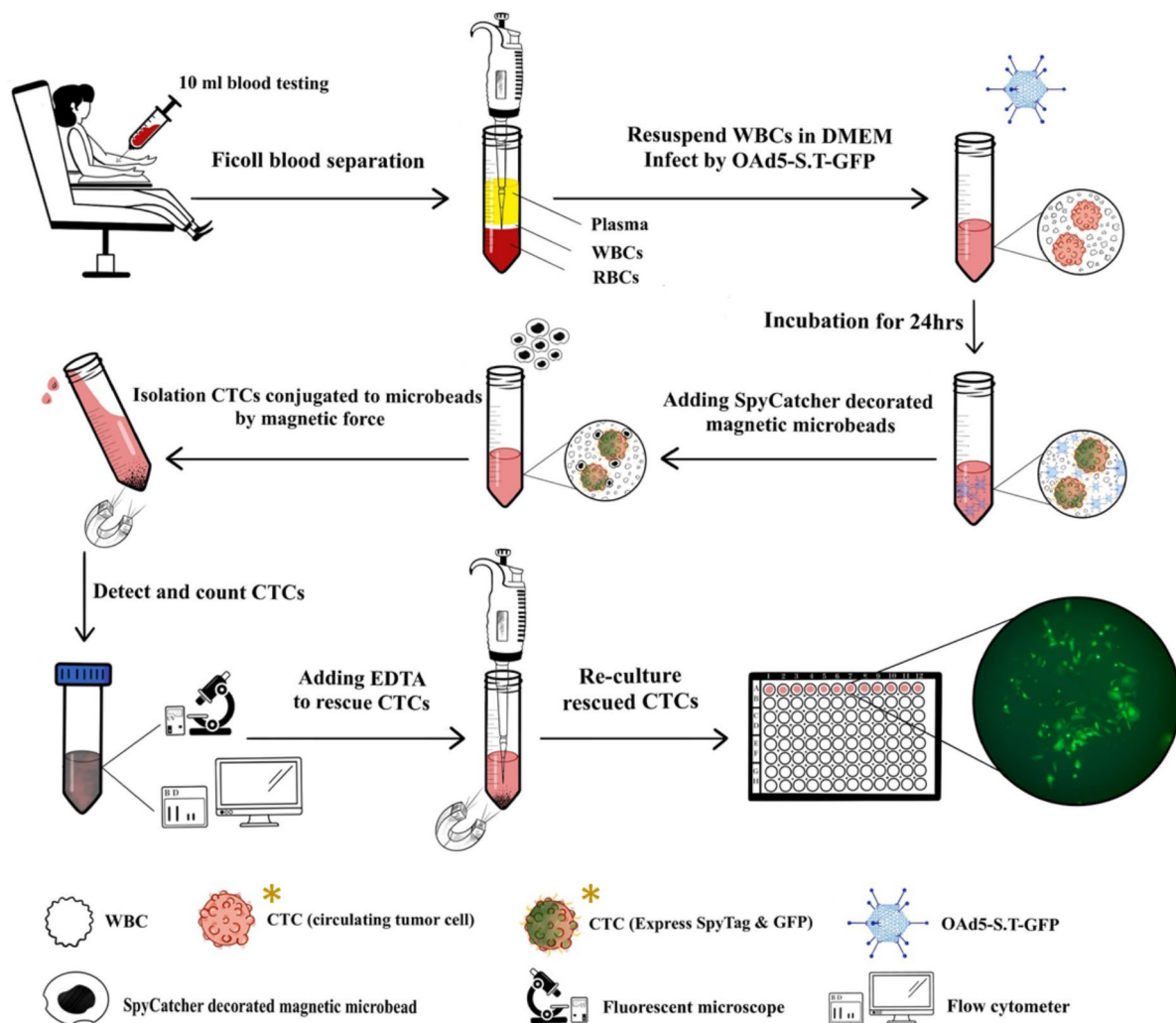


Fig. 1. Schematic Diagram of clinical vision for detection, isolation, and re-culture of tumor cells by CR-Ad5-ST-GFP and SpyCatcher decorated magnetic beads. *In this study, spiked cancer cell lines (A549, MCF7 and Ca Ski) were used as a model for the CTCs.

qPCR. Cytopathic effects and comet-like GFP colonies indicated successful replication in telomerase-positive cells.

Cell-based ELISA for spytag detection on the surface of infected cells

The expression of SpyTag on infected cells was confirmed via ELISA (BioTek, ELx800, USA). A-549 cells infected with CR-Ad5-ST-GFP were fixed and treated with 10 μ M SpyCatcher protein derived from a previous study¹⁶, followed by anti-SpyCatcher serum¹⁶ and an HRP-conjugated secondary antibody (Abcam Cat# ab34961, RRID: AB_732996). The absorbance was measured at 450 nm to quantify SpyTag presentation. Statistical analyses were performed using GraphPad Prism by the ordinary one-way ANOVA test.

Detection of CTCs by CR-Ad5-ST-GFP

Peripheral blood mononuclear cells (PBMCs) were isolated from 10 mL of blood collected from a healthy donor using Ficoll (Sigma-Aldrich, USA) density gradient centrifugation. Tumor cells (A-549, MCF-7, and Ca Ski) were spiked into PBMCs at various ratios (1:10, 1:100, 1:1000, and 1:10,000 and infected with CR-Ad5-ST-GFP (MOI of 10). After incubation for 24–48 h, GFP-expressing tumor cells were detected using flow cytometry (CyFlow, Partec, Germany) and fluorescence microscopy. To ensure accurate quantification, dead cells and debris were excluded by gating based on forward scatter (FSC) and side scatter (SSC) characteristics. Only intact single cells were selected for further analysis, and GFP-positive cells were quantified. The detailed gating strategy, including FSC-SSC gating for intact cell selection and GFP-positive gating, is provided in Supplementary Section S5 (Supplementary Figure S8 and S9). All recovery rates were reported after subtracting the standard deviation of the negative control (Ctrl(-)) and PBMC background signal. The experimental protocol was reviewed

and approved by the Ethics Committee at Iran Institute of Pasteur (Approval ID: IP.PII.REC.1399.011). All experiments were conducted in accordance with relevant institutional guidelines and regulations.

Preparation and characterization of SpyCatcher-decorated agarose magnetic beads

SpyCatcher protein was expressed and purified as described in our previous study¹⁶. Agarose magnetic microbeads were then decorated with a SpyCatcher to facilitate CTC isolation. Finally, SpyCatcher was incubated with microbeads for 3 h, and SpyCatcher decoration on agarose magnetic beads was investigated using ELISA, dynamic light scattering (DLS), and field emission scanning electron microscopy (FE-SEM). The complete preparation and characterization (FTIR and H-NMR) of agarose magnetic beads are detailed in Supplementary Materials (Section S2). Statistical analyses on ELISA absorbance at 450 nm were performed using GraphPad Prism. An unpaired two-tailed t-test was used to compare SpyCatcher binding between modified and unmodified beads. Data are presented as mean \pm SD.

Isolation of infected cancer cells with CR-Ad5-ST-GFP via spysystem

To assess the ability of SpyTag-SpyCatcher chemistry to isolate tumor cells, two approaches were used. In the first method, a 96-well plate was coated with modified agarose containing nickel ions bound to SpyCatcher, and null agarose was used as a control. They were incubated with infected A-549 cells, leading to the formation of agarose linked to SpyCatcher. Following a 2 h incubation, the wells were washed with PBS, and the washed waste from each well was examined by flow cytometry to determine the number of cells bound to SpyCatcher-decorated agarose. The samples were examined using fluorescence microscopy.

In the second method, modified magnetic microbeads were employed to isolate serially diluted infected A-549 cells from a population of one million PBMCs (1:10,000, 3:10,000, 5:10,000, and 10:10,000) to simulate the CTC isolation mechanism from the patient's blood in comparison to magnetic microbeads without SpyCatcher. The ability of SpyCatcher-decorated magnetic microbeads to capture tumor cells was subsequently evaluated using flow cytometry and fluorescence microscopy. Flow cytometry analysis of isolated cells was conducted; however, FSC-SSC gating was not applicable due to changes in particle size and granularity following cell binding to magnetic beads. The FL1-positive gating strategy described in “Detection of CTCs by CR-Ad5-ST-GFP” was applied to the magnetic microbeads, which were magnetically isolated and washed three times to remove unattached cells and debris. Detailed gating steps are provided in Supplementary Section S5 (Supplementary Fig. S10).

Re-culture of isolated tumor cells

To expand the isolated cancer cell line, 10^4 A-549 cells were spiked with 10^6 PBMCs and infected with CR-Ad5-ST-GFP at an MOI of 10. Cancer cells isolated using magnetic beads were released using 1 mM EDTA (Biosera, France), which chelates Ni^{2+} ions without harming the cells. The recovered cells were re-seeded into culture plates with DMEM containing 10% FBS and incubated for 10 days. Microscopy confirmed cell viability, adherence, and proliferation. Colonies expressing GFP were observed within 48 h and monitored for expansion over time.

Results

CR-Ad5-ST-GFP development

To target adenovirus replication to cancer cells, the hTERT promoter was utilized to drive E1A gene expression, exploiting its strong activity in cells with high telomerase levels (Fig. 2A). This enabled selective viral replication in cancer cells¹⁷. For detecting and isolating circulating tumor cells (CTCs), the EGFP gene served as a reporter, while the SpyTag-Fc-TM sequence facilitated binding to SpyCatcher-decorated magnetic beads. Both the EGFP and SpyTag-Fc-TM genes were inserted into the E3 region of pAdEasy-1 under separate CMV promoters (Fig. 2B), ensuring robust and efficient expression of both genes.

Following virus rescue, the replication specificity of CR-Ad5-ST-GFP was tested in A-549 cells. Unlike non-replicative adenoviruses, which cannot multiply in normal cells except for 293AD (a cell line with E1 complement genes), CR-Ad5-ST-GFP, containing the hTERT-E1A construct, replicated exclusively in cancer cells¹⁸. Introducing the virus into A-549 cells at an MOI of 10 resulted in comet-like cytopathic effects (CPEs) with GFP expression after 48 h, indicative of active viral replication. Over time, these colonies expanded due to continued viral proliferation (Fig. 2C). Quantitative PCR further confirmed this, showing a 100-fold and 500-fold increase in viral titers at 48 and 96 h, respectively. This demonstrated the virus's replication capability and cancer-cell specificity.

Identification of spytag on the surface of infected A-549 cells

The SpyTag peptide was engineered for surface expression by incorporating the CMV-SpyTag-Fc-TM construct into the E3 region of the CR-Ad5-ST-GFP genome to enable CTC isolation. Binding assays, ELISA absorbance at 450 nm, demonstrated significantly stronger interactions between infected A-549 cells and SpyCatcher/anti-SpyCatcher serum compared to controls, confirming successful SpyTag surface expression ($n=3$, $P<0.0001$). This facilitated the effective targeting and binding of CTCs (Supplementary Fig. S6). Additional experimental details can be found in the Supplementary Materials (Supplementary Sect. S3).

Detection of cancer cell lines via CR-Ad5-ST-GFP

To evaluate the effectiveness of CR-Ad5-ST-GFP in detecting individual cancer cells within a large PBMC population, various tumor cell types (A-549, MCF-7, and Ca Ski) were spiked into 1 million PBMCs and subsequently infected with the virus. Detection efficiency varied by tumor cell type and spiking ratio, with A-549, MCF-7, and Ca Ski cells showing different levels of alignment between the expected and observed recovery

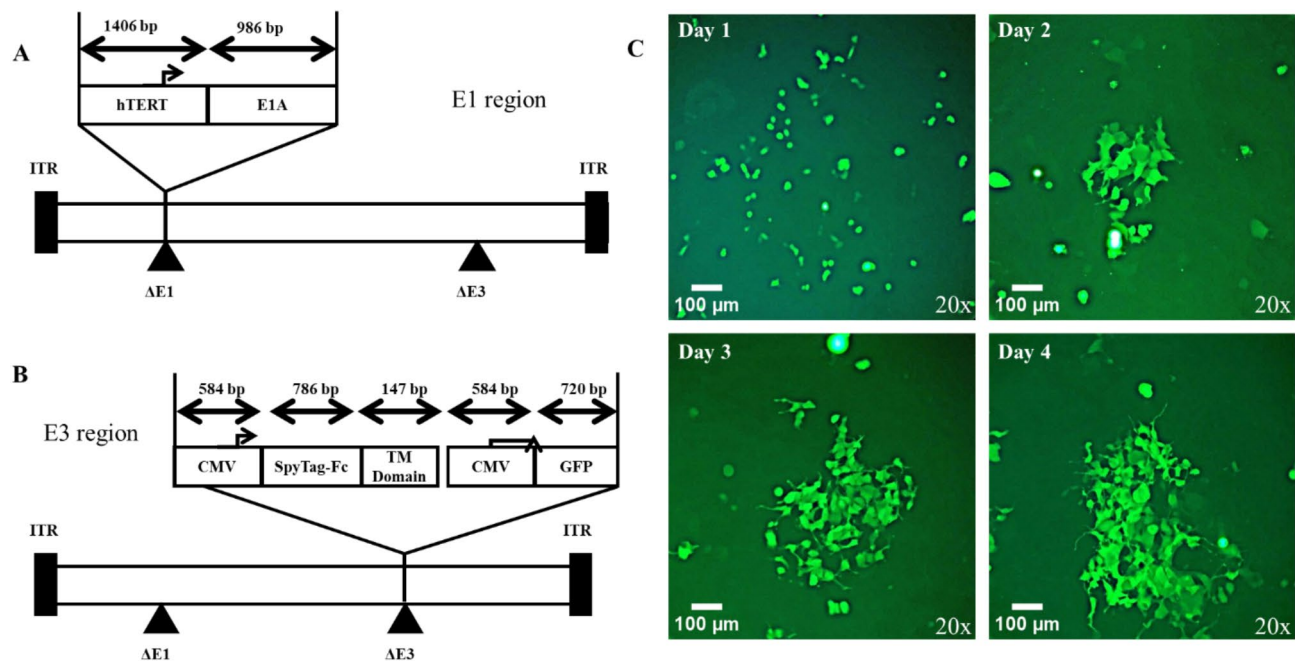


Fig. 2. (A) The genomic structure of CR-Ad5-ST-GFP, which contains the E1A gene but lacks E1B under the control of the hTERT promoter. (B) CR-Ad5-ST-GFP expresses SpyTag-Fc and GFP in the E3 region. (C) CR-Ad5-ST-GFP replicates in A-549 cells, as evidenced by the formation of GFP-expressing comet-like CPE and increased colony size over time.

Spiked cells (ratio % per 1 million PBMCs)		100,000 (10%)	10,000 (1%)	1000 (0.1%)	100 (0.01%)	SD of Cntrl (-)
Detected cells (recovery rate %)	A549	85,600 (85.2%)	10,400 (100%)	1,500 (≈ 100%)	500 (≈ 100%)	200
	MCF-7	29,800 (29.4%)	4,600 (42%)	1,700 (≈ 100%)	400 (0%)	
	Ca Ski	85,600 (85.2%)	11,800 (≈ 100%)	1,500 (≈ 100%)	900 (> 100%)	
	PBMC	-	-	-	-	

Table 1. The proportions of detected tumor cells (A-549, Ca ski, and MCF-7) after infection with CR-Ad5-ST-GFP at MOI of 10 after 24 h, following their introduction to PBMCs at different ratios.

rates. Flow cytometry results (Table 1; Fig. 3A) revealed a general trend of reduced detection efficiency as the number of spiked tumor cells decreased. A-549 and Ca Ski cells demonstrated a strong correlation between the spiked and recovered cell numbers across 100,000, 10,000, and 1000 spiking levels. In contrast, MCF-7 cells exhibited consistently lower recovery rates at these levels. At the 100-cell spiking concentration, A-549 cells exhibited a detection rate consistent with the expected recovery. However, Ca Ski cells showed a recovery rate higher than anticipated. MCF-7 cells, however, showed no detectable cells after adjusting for the standard deviation of the negative control (Cntrl (-)) and accounting for false-positive signals from PBMCs. Despite the variations in recovery rates, CR-Ad5-ST-GFP successfully detected tumor cells across all spiking levels, with notable differences between cell types. Furthermore, PBMCs infected with CR-Ad5-ST-GFP showed negligible infection, further confirming the virus's specificity for cancer cells (Fig. 3B). Fluorescence microscopy further validated the sensitivity of the detection method, demonstrating that even 100 spiked tumor cells could be reliably detected within a population of 1 million PBMCs (Fig. 3C).

Engineering SpyCatcher-decorated agarose magnetic beads

To isolate SpyTag-expressing cancer cells, SpyCatcher proteins were conjugated to nickel-chelated magnetic agarose beads. The chemical activation and functionalization of the beads were confirmed through FT-IR and H-NMR analyses, which verified the successful incorporation of iminodiacetic acid (IDA) onto the agarose matrix. Chelation with nickel ions was visually validated by a distinct blue shift in the bead solution's hue. These functionalized beads were used to isolate cells expressing SpyTag on their surfaces (Fig. 4A). The functionality of SpyCatcher-decorated beads was examined using FE-SEM, DLS, and ELISA. FE-SEM images (Fig. 4B) showed that the spherical structure of the magnetic microbeads was maintained after SpyCatcher conjugation, with only a slight increase in surface roughness. DLS analysis revealed an increase in bead size from 1124 ± 61 nm to 2211 ± 105 nm following SpyCatcher conjugation (Fig. 4C). The optimal size range of 1–5 μm for CTC isolation was achieved, minimizing contamination from smaller blood cells while preserving CTC viability. Additionally,

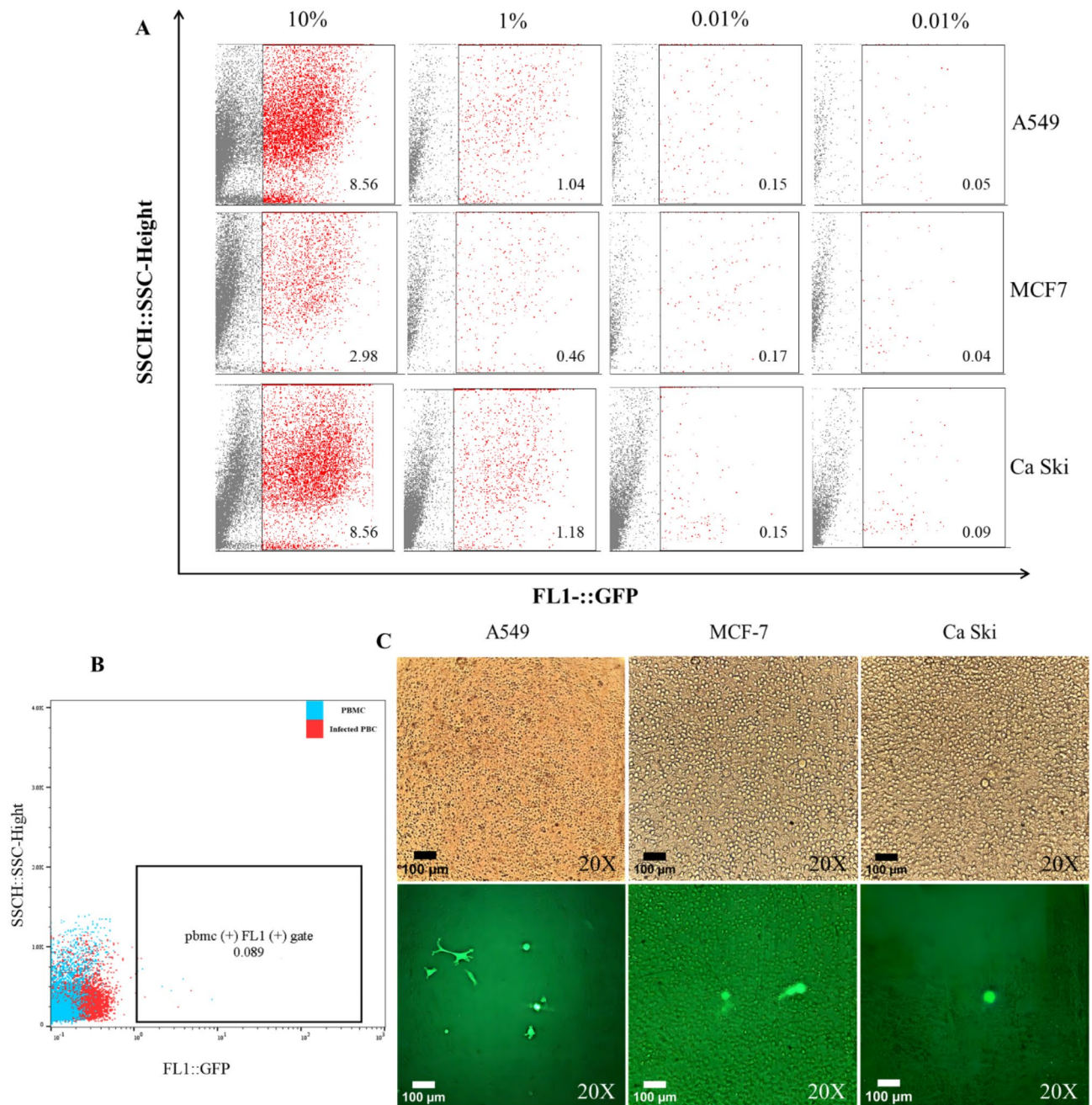


Fig. 3. Evaluation of detection potency via flow cytometry and fluorescence microscopy. **(A)** SSC-FL1 graphs of A-549, MCF-7, and Ca Ski cells infected with CR-Ad5-ST-GFP. The ratio of detected cells per 1 million PBMCs is reported as percentages at each spiking ratio. **(B)** Flow cytometry analysis of PBMCs infected with CR-Ad5-ST-GFP. **(C)** Bright-field and fluorescent microscopy images of CR-Ad5-ST-GFP-infected tumor cells (A549, MCF-7 and Ca Ski) in PBMCs (0.01% spiking ratio and $\times 20$ magnification). Bright-field images showing the morphology of the cells. Corresponding fluorescent images demonstrating GFP expression in infected cells.

the polydispersity index (PDI) of the beads increased from 0.7 to 1 after SpyCatcher decoration, indicating slight variability in particle size. ELISA results (Fig. 4D) further confirmed SpyCatcher binding to the bead surface, as anti-His HRP-conjugated antibodies demonstrated strong interactions with SpyCatcher-coated beads (1.85 ± 0.1) compared to unmodified beads (0.68 ± 0.07). This confirmed the successful functionalization of the magnetic beads for efficient CTC isolation ($n=3$, $p<0.0001$).

Capture of tumor cells through the SpyTag–SpyCatcher interaction

To assess the efficiency of the agarose-IDA-Ni²⁺-SpyCatcher system in isolating tumor cells expressing SpyTag, A-549 cells infected with CR-Ad5-ST-GFP were introduced to wells containing SpyCatcher-decorated agarose

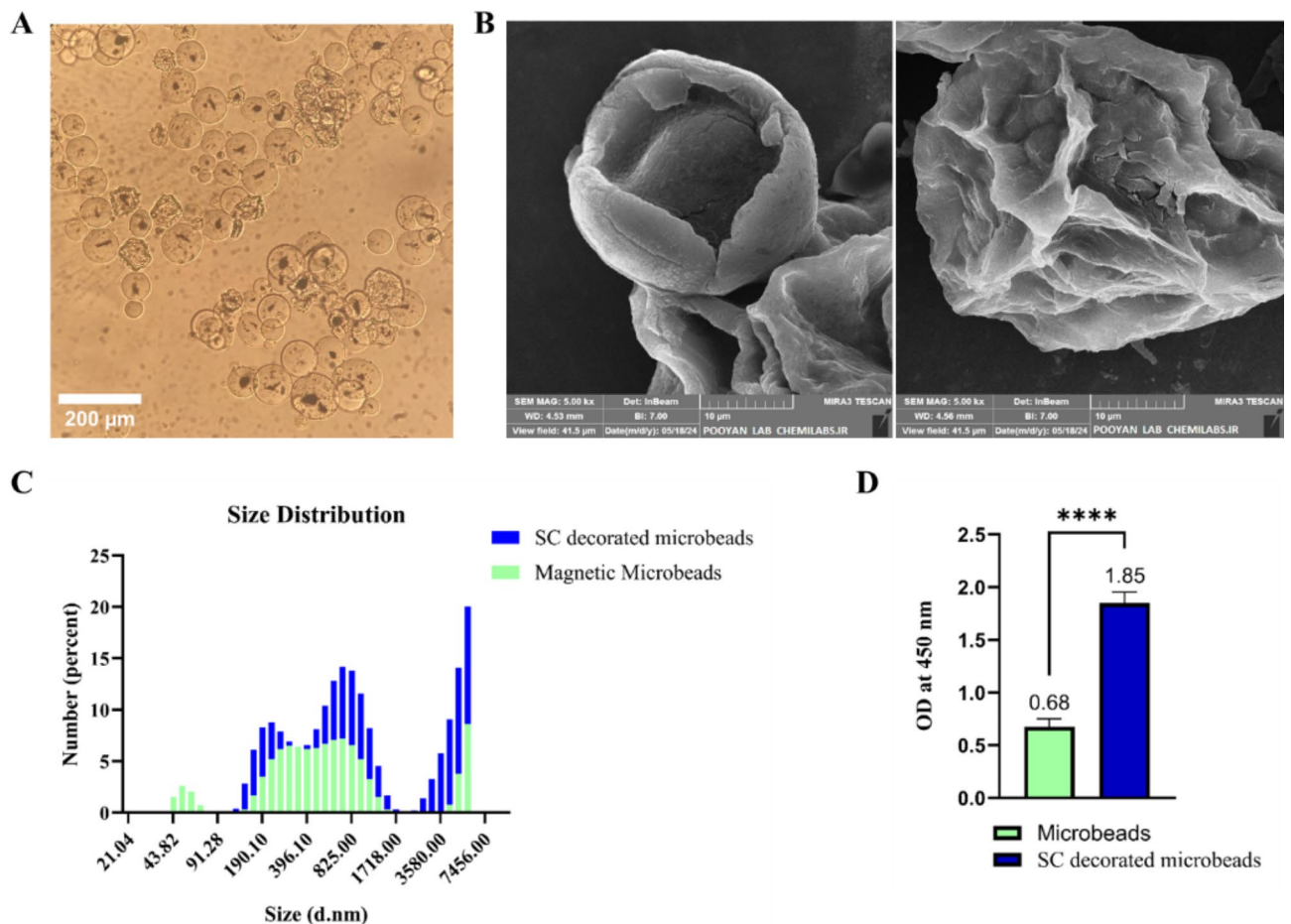


Fig. 4. Characterization of SpyCatcher-decorated magnetic microbeads. (A) Microscopy images. (B) FE-SEM images of intact agarose magnetic microbeads (left) and SpyCatcher-decorated magnetic microbeads (right). (C) Particle size analysis. (D) ELISA results. Agarose magnetic microbeads were added to each well of a 96-well plate. The microbeads were fixed, blocked, and then incubated with an anti-His HRP-conjugated antibody. After washing, TMB was added, followed by the addition of a stop solution. The absorbance was measured at 450 nm. Error bars represent standard deviation ($n = 3$), $p < 0.0001$ unpaired t-test.

and uncoated null agarose as controls (Fig. 5A,B). The same number of infected A-549 cells bound to the SpyCatcher-decorated agarose (Fig. 5A,B), though a small number of GFP-expressing A-549 cells were detected in the wash from the SpyCatcher-decorated agarose (Fig. 5C). Fluorescence microscopy images (Fig. 5D,E) showed that untreated agarose did not capture infected A-549 cells after washing with PBS. The wash from the null agarose contained nearly the same number of infected cells as were initially added (Fig. 5F), confirming the specificity of the SpyCatcher-functionalized beads for capturing infected cells.

Secondly, A-549 cells were spiked with PBMCs at various ratios (100:1 million, 300:1 million, 500:1 million, and 1,000:1 million) and infected with CR-Ad5-ST-GFP. The mixture was then combined with SpyCatcher-decorated agarose magnetic beads. As shown in Fig. 6A, more than 50% of A-549 cells were detected at a 1000:1 million spiking ratio, and recovery rate increased to 80% as the number of A-549 cells decreased relative to the constant number of PBMCs. The Limit of Detection (LOD) for this assay was calculated to be approximately 35 cells per 10^6 PBMCs (Supplementary Sect. S4), indicating the sensitivity of the method in detecting low numbers of A-549 cells. Fluorescence microscopy images (Fig. 6B) confirmed that A-549 cells were successfully captured on the microbeads, consistent with the flow cytometry results.

Re-culture of isolated cancer cells

To evaluate the viability of isolated cells for in vitro cultivation, 10^4 A-549 infected cells were co-incubated with 10^6 PBMCs and isolated using SpyCatcher-decorated magnetic microbeads. The cells were separated from the beads using EDTA and replanted for 10 days. As shown in Fig. 7, cells adhered to the surface within 24 h, as seen in 40× microscopy images. Higher-magnification images (Fig. 7A) revealed a morphological transition from a spherical to a star-like shape after 48 h, confirming the feasibility of re-culturing the isolated cells. Despite viral infection and replication, A-549 cells retained normal attachment to the wells. At 48-h intervals, the cells were examined for proliferation, and after five days, some cells began to proliferate and expand. Over time, A-549 cells

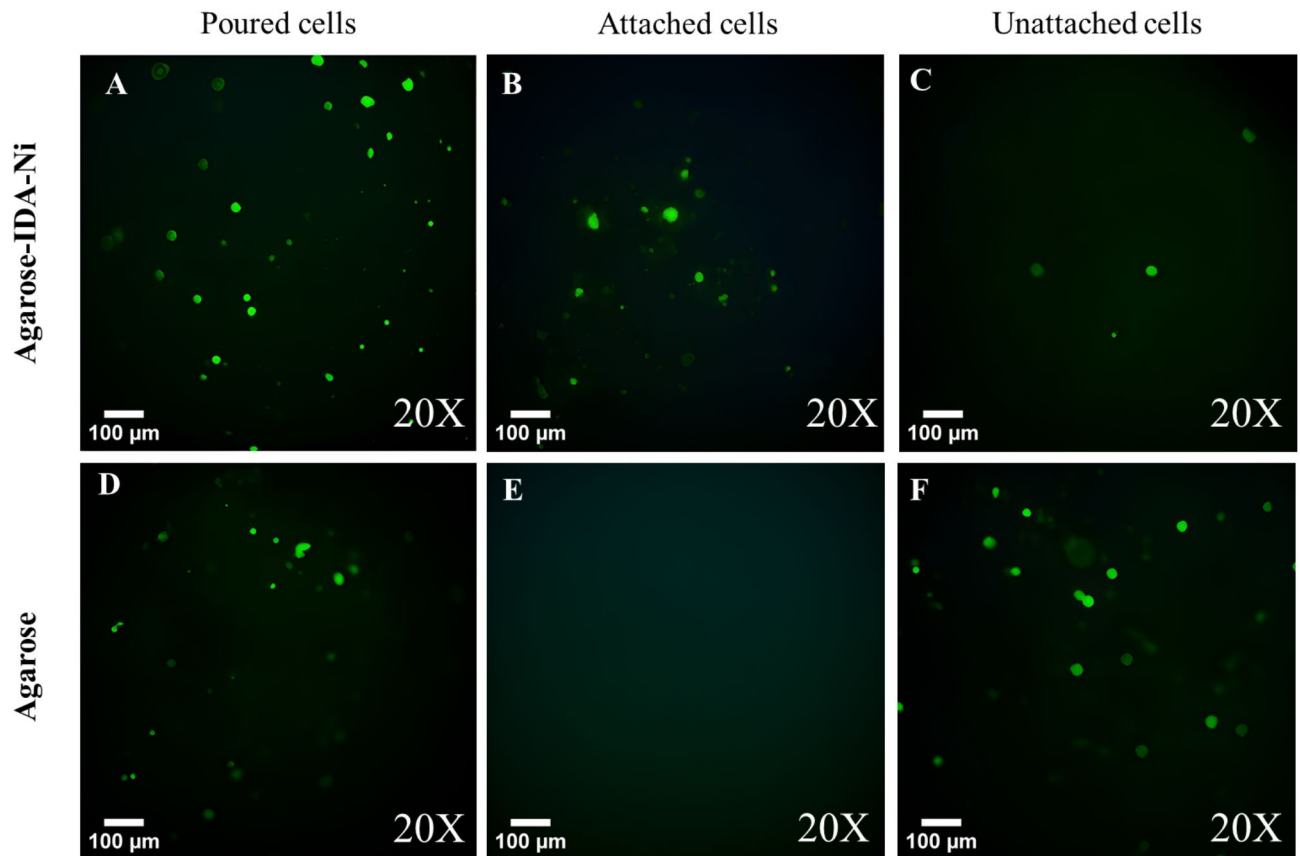


Fig. 5. Infected cells attached to SpyCatcher-decorated agarose versus control agarose. The cells were added to SpyCatcher-depleted and control wells (A,D). The cells were observed after the wells were washed with PBS (B,E). The cells were collected by washing with PBS as the flow-through from the other wells (C,F).

formed small colonies expressing GFP, indicating viral replication. While viral replication slowed cell growth and division, infected cells still proliferated (Fig. 7B).

Discussion

Detecting CTCs presents considerable challenges, particularly due to their rarity and phenotypic heterogeneity^{4,5}. Traditional CTC detection approaches often rely on antibody-based techniques targeting epithelial markers such as EpCAM. However, these methods have notable limitations, especially during EMT, where epithelial markers are downregulated, resulting in false negatives⁷. Furthermore, many existing platforms fail to preserve the viability of isolated cells, restricting their downstream utility for molecular analysis and drug sensitivity testing^{10,19}. Our study sought to address these challenges by developing a novel system combining a conditionally replicative adenovirus (CR-Ad5-ST-GFP) with the SpyTag/SpyCatcher system to enhance the detection, isolation, and recovery of viable CTCs.

The CR-Ad5-ST-GFP virus utilized selectively replicates in telomerase-positive tumor cells, driven by the hTERT promoter, ensuring minimal activity in normal blood cells¹⁷. This selective replication not only minimizes background interference from white blood cells (WBCs) but also enables the identification of viable CTCs through GFP expression, which is inherently linked to viral replication. Unlike surface marker-based methods, our system circumvents the issue of EMT-induced marker loss, allowing for more comprehensive detection of CTC subpopulations^{12,20}. Additionally, GFP expression facilitates the quantification of CTCs via flow cytometry and fluorescence microscopy, providing a sensitive and robust detection modality²¹.

To isolate CTCs, we engineered the CR-Ad5-ST-GFP virus to express SpyTag on the surface of infected cells. SpyTag forms a stable covalent bond with SpyCatcher, enabling robust and efficient isolation of infected cells. The use of SpyCatcher-functionalized magnetic agarose beads further enhanced this system's efficacy. Detailed characterization of these beads, including SEM, DLS, and ELISA analyses, confirmed the successful conjugation of SpyCatcher and demonstrated their suitability for capturing SpyTag-expressing cells^{14,15}. Importantly, our system achieved an isolation efficiency (recovery rate) exceeding 80% when detecting A-549 or Ca Ski cells spiked into peripheral blood mononuclear cells (PBMCs). Even at low spiking ratios, such as one CTC per 10,000 PBMCs, our method has potential to be highly sensitive and specific.

The calibration curve demonstrates a strong correlation ($R^2 = 0.9993$) between the number of spiked cancer cells and detected cells, indicating the reliability of the assay (Supplementary Table S2 and Supplementary Fig. S7). The calculated LOD of ~ 35 cells per 10^6 PBMCs supports the method's sensitivity. While this result shows

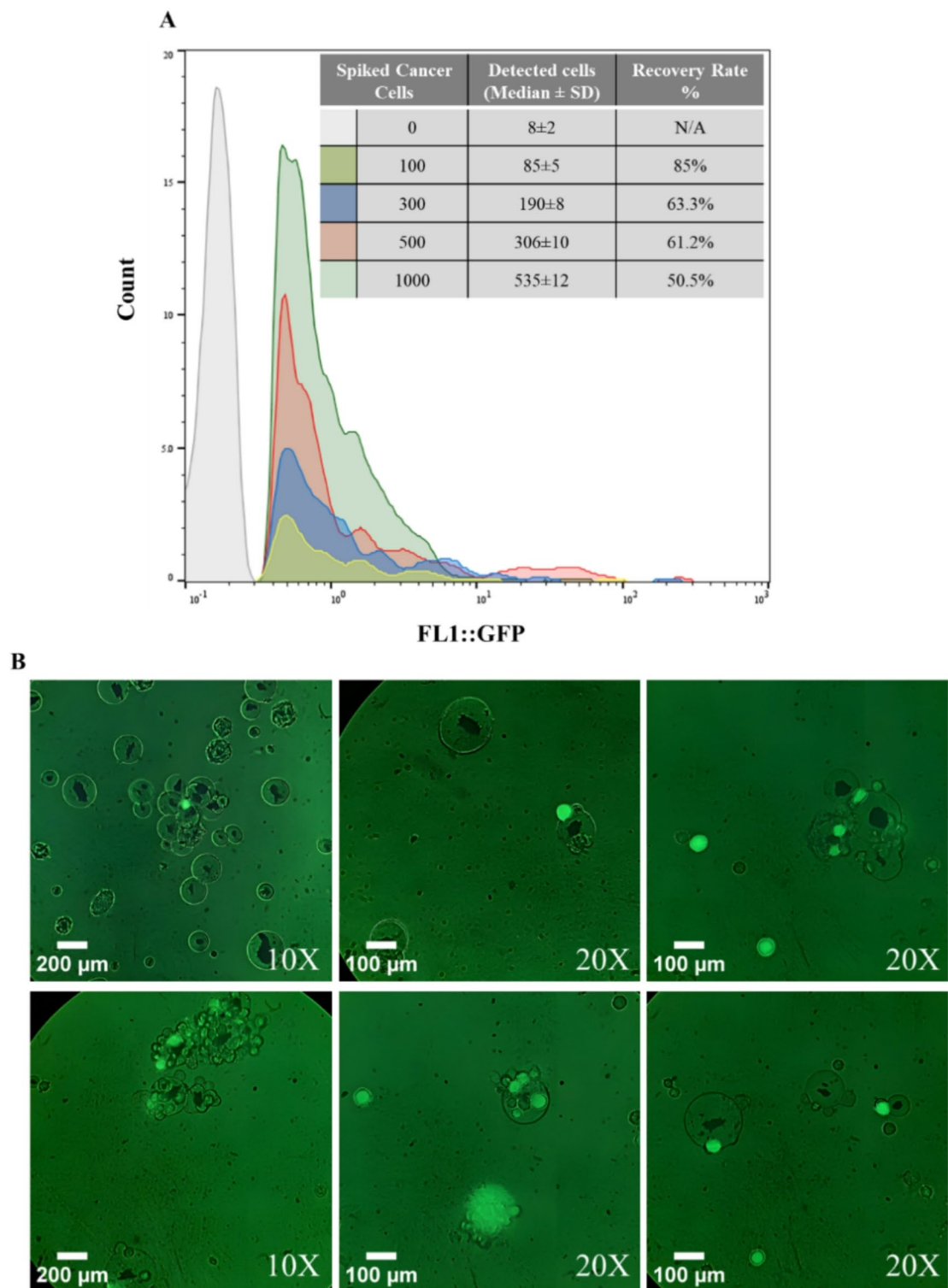


Fig. 6. Isolation of infected cells via SpyCatcher-decorated magnetic microbeads. **(A)** Flow cytometry results of A-549-spiked cells (100, 300, 500, and 1000 cells) in 1 million PBMCs. **(B)** Six fields of microscopic images that show the cells bonded to the microbeads through the SpyCatcher–SpyTag system.

promising, further refinement and clinical validation are required to achieve the detection of a single CTC per 10^6 WBCs.

One of the critical advantages of our approach is the ability to recover viable CTCs. In our system, we overcame this by using 1 mM EDTA, which known as a chelating agent efficiently detaches cancer cells conjugated to SptCatcher from the Ni^{2+} covered agarose beads without compromising their viability, allowing for subsequent

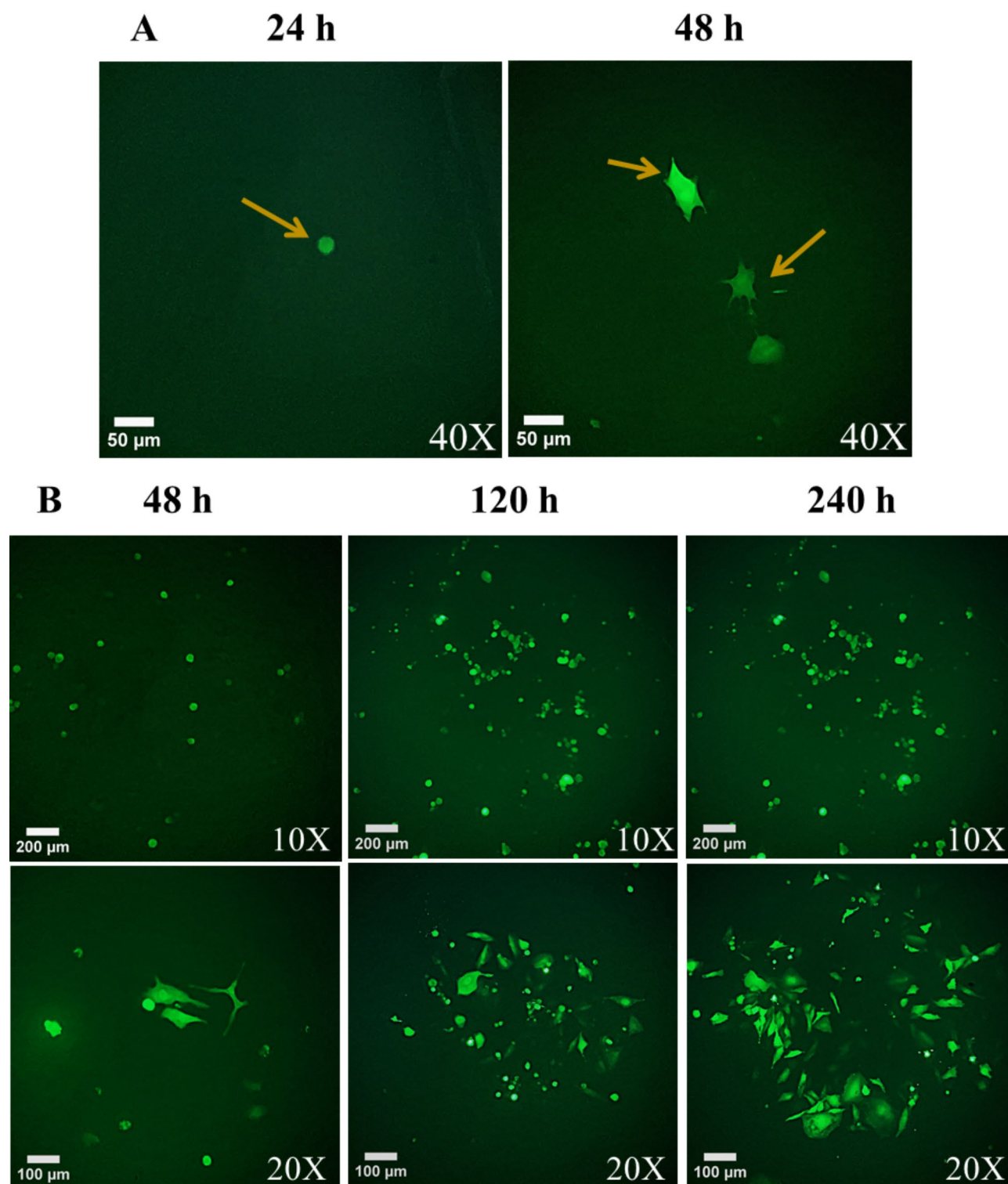


Fig. 7. Re-culturing of isolated cells: (A) Fluorescence microscopy images of cells at 48 h. (B) Fluorescence microscopy images of cell colonies over time.

culturing and analysis²². Although viral replication slowed cell growth and division, re-culturing experiments showed that isolated A-549 cells adhered to culture plates, maintained normal morphology, and formed colonies expressing GFP. This is because our virus is less lytic as the E1 gene is regulated by the hTERT promoter. This is particularly important for investigating the genetics and epigenetics of CTCs, which could provide valuable insights for personalized cancer therapies^{23,24}.

While our system demonstrated robust performance, some limitations should be noted. The discrepancies observed in the detection efficiency of MCF-7 cells highlight the need for further optimization, particularly for tumor cell lines with lower adenovirus susceptibility. Additionally, the lack of patient-derived samples in this study limits the immediate clinical applicability of our findings. Future studies should incorporate clinical samples to validate the performance of our platform under more realistic conditions²⁵. Furthermore, the constant number of magnetic beads used across varying cell concentrations suggests that optimization of bead-to-cell ratios could enhance isolation efficiency.

The compatibility of our system with advanced technologies, such as microfluidics, presents exciting opportunities for high-throughput CTC detection and isolation. By integrating our approach into automated microfluidic platforms, it may be possible to achieve real-time CTC monitoring in clinical settings, enabling personalized cancer therapy and early detection of metastasis^{1,26}.

In summary, this study introduces an innovative platform that combines tumor-selective adenoviral replication with the SpyTag/SpyCatcher system to detect, isolate, and recover viable CTCs. This method addresses key limitations of existing approaches, offering a robust solution for comprehensive CTC analysis. Future work should focus on clinical validation and optimizing system parameters to fully realize the potential of this technology in cancer diagnostics and treatment.

Conclusion

We developed an innovative technique that combined crAD with the SpyTag/SpyCatcher system to effectively identify and retrieve viable CTCs. This proof-of-concept study revealed that this method can be used in the future to monitor tumor progression, predict patient prognosis, and evaluate the therapeutic efficacy of individualized treatments. This is the first study to demonstrate that a tumor-selective replicating adenovirus expressing GFP and SpyTag combined with an immobilized SpyCatcher agarose magnetic bead can efficiently identify and isolate living CTCs, allowing them to be re-cultured for further analyses or experiments. The ability of our approach to re-culture living CTCs is remarkable because it allows for the expansion and investigation of these rare cells, thereby revealing important new information on cancer development, drug efficacy, and patient prognosis. Additionally, this study not only advances the utility of crAD-based platforms but also demonstrates the feasibility of integrating novel molecular interaction systems like SpyTag/SpyCatcher with adenoviral vectors. The platform's compatibility with emerging technologies such as microfluidics further enhances its potential for high-throughput, automated detection and isolation of CTCs in clinical settings.

Data availability

The data supporting the findings of this study are available from the Pasteur Institute of Iran (Virology Department) upon request. Additional data supporting the findings of this study are available from the corresponding author upon reasonable request.

Received: 25 December 2024; Accepted: 24 March 2025

Published online: 02 April 2025

References

- Lin, D. et al. Circulating tumor cells: biology and clinical significance. *Signal. Transduct. Target. Ther.* **6**, 404 (2021).
- Alix-Panabières, C. & Pantel, K. Circulating tumor cells: liquid biopsy of cancer. *Clin. Chem.* **59**, 110–118 (2013).
- Lawrence, R., Watters, M., Davies, C. R., Pantel, K. & Lu, Y. J. Circulating tumour cells for early detection of clinically relevant cancer. *Nat. Rev. Clin. Oncol.* **20**, 487–500 (2023).
- Yang, Y. et al. Circulating tumour cell clusters: isolation, biological significance and therapeutic implications. *BMJ Oncol.* **3**, e000437 (2024).
- Prieto-García, E., Díaz-García, C. V., García-Ruiz, I. & Agulló-Ortuño, M. T. Epithelial-to-mesenchymal transition in tumor progression. *Med. Oncol.* **34**, 1–10 (2017).
- Habli, Z., AlChamaa, W., Saab, R., Kadara, H. & Khraiche, M. L. Circulating tumor cell detection technologies and clinical utility: Challenges and opportunities. *Cancers (Basel)*. **12**, 1930 (2020).
- Brown, T. C., Sankpal, N. V. & Gillanders, W. E. Functional implications of the dynamic regulation of EpCAM during epithelial-to-mesenchymal transition. *Biomolecules*. **11** (2021).
- Kanayama, M. et al. Enhanced capture system for mesenchymal-type circulating tumor cells using a polymeric microfluidic device 'CTC-Chip' incorporating cell-surface vimentin. *Oncol. Rep.* **52**, 156 (2024).
- Vidlarova, M. et al. Recent advances in methods for circulating tumor cell detection. *Int. J. Mol. Sci.* **24** (2023).
- Cheng, J. et al. Nanotechnology-assisted isolation and analysis of circulating tumor cells on microfluidic devices. *Micromachines*. **11** (2020).
- Takakura, M. et al. Circulating tumour cells detected by a novel adenovirus-mediated system May be a potent therapeutic marker in gynaecological cancers. *Br. J. Cancer*. **107**, 448–454 (2012).
- Kojima, T. et al. A simple biological imaging system for detecting viable human Circulating tumor cells. *J. Clin. Invest.* **119**, 3172–3181 (2009).
- Hu, M. et al. Advances in oncolytic herpes simplex virus and adenovirus therapy for recurrent glioma. *Front. Immunol.* **14**, 1285113 (2023).
- Brune, K. D. et al. Plug-and-display: decoration of virus-like particles via isopeptide bonds for modular immunization. *Sci. Rep.* **6**, 19234 (2016).
- Gilbert, C., Howarth, M., Harwood, C. R. & Ellis, T. Extracellular self-assembly of functional and tunable protein conjugates from *Bacillus subtilis*. *ACS Synth. Biol.* **6**, 957–967 (2017).
- Kadkhodazadeh, M. et al. Fiber manipulation and post-assembly nanobody conjugation for adenoviral vector retargeting through SpyTag-SpyCatcher protein ligation. *Front. Mol. Biosci.* **9**, 1039324 (2022).
- Liu, M. et al. The regulations of telomerase reverse transcriptase (TERT) in cancer. *Cell. Death Dis.* **15**, 90 (2024).
- Leikas, A. J., Ylä-Herttua, S. & Hartikainen, J. E. K. Adenoviral gene therapy vectors in clinical Use—Basic aspects with a special reference to Replication-Competent adenovirus formation and its impact on clinical safety. *Int. J. Mol. Sci.* **24**, 16519 (2023).
- Castro-Giner, F. & Aceto, N. Tracking cancer progression: from circulating tumor cells to metastasis. *Genome Med.* **12**, 31 (2020).

20. Xu, Y. et al. Circulating tumor cells (CTCs) and hTERT gene expression in CTCs for radiotherapy effect with lung cancer. *BMC Cancer*. **23**, 475 (2023).
21. Xu, M. J. et al. A novel approach for the detection and genetic analysis of live melanoma Circulating tumor cells. *PLoS One*. **10**, e0123376 (2015).
22. Lau, E. C. H. T. et al. Direct purification and immobilization of his-tagged enzymes using unmodified nickel ferrite NiFe₂O₄ magnetic nanoparticles. *Sci. Rep.* **13**, 21549 (2023).
23. Li, C. et al. Application of microfluidics in detection of circulating tumor cells. *Front. Bioeng. Biotechnol.* **10**, 907232 (2022).
24. Sharma, S. et al. Circulating tumor cell isolation, culture, and downstream molecular analysis. *Biotechnol. Adv.* **36**, 1063–1078 (2018).
25. Ikemoto, S. et al. Novel conditionally replicating adenovirus-mediated efficient detection of Circulating tumor cells in lung cancer patients. *PLoS One*. **18**, e0286323 (2023).
26. Ma, Y. et al. A combinatory strategy for detection of live CTCs using microfiltration and a new telomerase-selective adenovirus. *Mol. Cancer Ther.* **14**, 835–843 (2015).

Acknowledgements

The authors express their gratitude to Dr. Mahsa Rasekhian and Dr. Nasir Mohajel for their technical assistance. They also acknowledge the valuable contributions of Mrs. Farnaz Nematzadeh, who created the illustrations for the figures. The authors thank the Pasteur institute of Iran funding Dr. Kayhan Azadmanesh's research (Grant 1768). There are no conflicts of interest to declare.

Author contributions

S.G. and K.A. and M.K. conceptualized and designed the study. S.G. performed the experiments, collected the data, and analysed the results. S.G. contributed to the development and optimization of the SpyTag/SpyCatcher and adenoviral systems. S.G. and K.A. provided critical technical expertise in flow cytometry and fluorescence microscopy. K.A., M.Kh. and S.H.J. supervised the project, provided resources, and guided the experimental design. S.G. and M.K. wrote the manuscript, with revisions (included K.A. and M.KH.) and intellectual input from all authors. All authors reviewed and approved the final manuscript.

Funding

The authors thank the Pasture Institute of Iran for funding Dr. Kayhan Azadmanesh's research (Grant 1768).

Declarations

Competing interests

The authors declare no competing interests.

Ethical approval

All procedures involving human participants were conducted in accordance with the ethical guidelines outlined in the IP.PII.REC.1399.011. Written informed consent was obtained from healthy female donors (age: 37 years) before the collection of PBMCs. This study complied with all the relevant ethical principles.

Additional information

Supplementary Information The online version contains supplementary material available at <https://doi.org/10.1038/s41598-025-95671-x>.

Correspondence and requests for materials should be addressed to K.A.

Reprints and permissions information is available at www.nature.com/reprints.

Publisher's note Springer Nature remains neutral with regard to jurisdictional claims in published maps and institutional affiliations.

Open Access This article is licensed under a Creative Commons Attribution-NonCommercial-NoDerivatives 4.0 International License, which permits any non-commercial use, sharing, distribution and reproduction in any medium or format, as long as you give appropriate credit to the original author(s) and the source, provide a link to the Creative Commons licence, and indicate if you modified the licensed material. You do not have permission under this licence to share adapted material derived from this article or parts of it. The images or other third party material in this article are included in the article's Creative Commons licence, unless indicated otherwise in a credit line to the material. If material is not included in the article's Creative Commons licence and your intended use is not permitted by statutory regulation or exceeds the permitted use, you will need to obtain permission directly from the copyright holder. To view a copy of this licence, visit <http://creativecommons.org/licenses/by-nc-nd/4.0/>.

© The Author(s) 2025